Multichannel Resonances in the Inelastic Scattering of Electrons by Helium

G. E. CHAMBERLAIN
National Bureau of Standards, Washington, D. C.
(Received 11 October 1966)

Resonance structure due to intermediate negative-ion states has been observed in the differential cross section for inelastic scattering of electrons at zero angle in helium. Resonances were observed in all four of the $1s \rightarrow 2s$, $2p$ channels within the incident-energy range of 19.5 to 24 eV.

I. INTRODUCTION

EARLIER measurements by Schulz[1] and Kuyatt *et al.*[2] of the elastic and total scattering cross sections for electrons on rare-gas atoms have shown the existence of resonance structure due to negative-ion states formed from excited atomic levels below the first ionization potential. Schulz and Philbrick[3] have shown that resonance structure is quite visible in the helium inelastic 2^3S loss channel at a scattering angle of 72°. Subsequently, resonances were observed for zero-angle scattering in all four of the helium $n=2$ inelastic channels.[4] This paper presents further details on the latter experiment.

II. APPARATUS AND ITS OPERATION

A. General Description

The apparatus has been described in detail elsewhere[2,5] and is shown schematically in Fig. 1. The monochromator is an energy selector for the primary electron beam entering the collision chamber and the analyzer is an energy selector for electrons leaving the collision chamber. Each energy selector was operated at a mean energy between 1 and 4 eV. Electrons enter and leave the collision chamber through two 0.5-mm diam apertures spaced 1.27-cm apart. The apertures used were constructed from 2.54-cm-diam molybdenum disks and were mounted in a stainless-steel holder. With provision for a gas inlet, this assembly constituted a differentially pumped gas cell with an 800:1 internal/external pressure ratio. The nominal operating pressure for helium was 50 mTorr.

The whole apparatus was operated inside an rf shielded enclosure and the earth's magnetic field was canceled with a single Helmholtz coil. At the gas-cell the residual component of magnetic field perpendicular to the energy dispersion plane was ~10 mG and the component in the dispersion plane and perpendicular to the electron beam was ~50–70 mG. However, since the angle-defining slits were oriented perpendicularly to the dispersion plane, the apparatus was less sensitive to the latter component of field. Subsequent to taking the data shown in Figs. 2 and 3 a cylinder of CoNetic magnetic shielding was installed inside the vacuum wall. The component of magnetic field in a plane perpendicular to the electron beam in the gas cell was reduced to less than 5 mG, but there was no noticeable change in the data.

Electrons from the analyzer were detected with a Faraday cup and vibrating-reed electrometer. The output of the electrometer was applied to the vertical scale of an X-Y recorder.

The helium gas used was commercial-grade, oil-free helium. No special cleaning procedures were employed other than periodically pumping out and refilling the gas-handling system.

B. Energy-Sweep Modes

There were two principal modes of operation for the electron spectrometer. In the energy-loss mode the energy of the primary beam was fixed and an energy-loss spectrum observed by varying the potential difference between the gas cell and analyzer. In the primary-energy mode the energy loss was fixed and the energy of the primary beam was varied. The latter mode is referred to as the transmission mode when the scattering angle and energy loss are zero. In the transmission

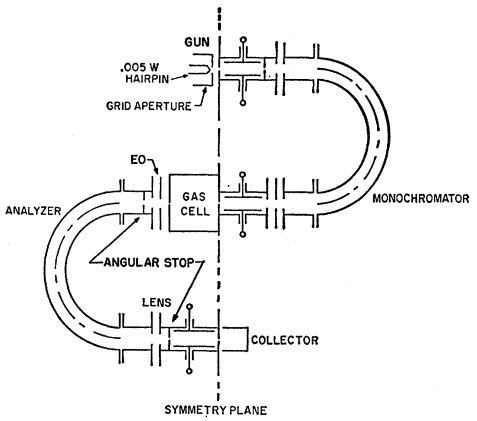

FIG. 1. Schematic diagram of electron spectrometer. The mean radius of both hemispherical velocity selectors is 2.540 cm. The double aperture lens consisted of 3.18-mm apertures spaced 3.18 mm apart. Beam defining apertures were 0.5-mm diam and angular stops were 0.5×1.5-mm slits except as noted in the text.

[1] G. J. Schulz, Phys. Rev. **136**, A650 (1964).
[2] C. E. Kuyatt, J. A. Simpson, and S. R. Mielczarek, Phys. Rev. **138**, A385 (1965).
[3] G. J. Schulz and J. W. Philbrick, Phys. Rev. Letters **13**, 477 (1964).
[4] G. E. Chamberlain and H. G. M. Heideman, Phys. Rev. Letters **15**, 337 (1965).
[5] J. A. Simpson, Rev. Sci. Instr. **35**, 1698 (1964).

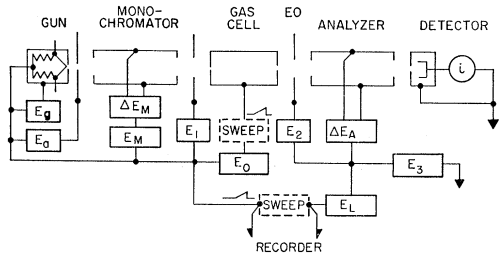

FIG. 2. Block diagram of electrical connections. E_0 and E_L were 0.01% regulated power supplies. E_g, E_M, $\Delta E_{A,M}$, the sweep generator, and the steering plate and filament voltages (not shown) were as described in Ref. 5. E_a and E_3 were regulated voltage supplies from which E_1 and E_2 were derived by potentiometer taps. The two positions for the sweep circuit shown were interchangeable by means of a four-pole, double-throw switch.

mode the observed current is exponentially dependent on the total cross section. For energy losses other than zero the observed current in the primary-energy mode is proportional to the differential cross section for inelastic scattering at zero angle.

The electrical connections for the apparatus are shown schematically in Fig. 2. Significant changes were made from previous methods of operation. Prior to the presently described experiments the anode, gas cell, and Faraday cup were fixed at the same (ground) potential. The apparatus was modified so that each stage of acceleration or deceleration operated independently of the others. One advantage of this type of operation was the simplification of the electron optics. After choosing the mean energies of the monochromator and analyzer and setting optimum values of the lens voltage ratios from gun to monochromator and from analyzer to Faraday cup, these parameters were left unchanged for either an energy-loss or a primary-energy sweep.[6]

Only the potential of the scattering chamber was changed for primary-energy sweeps. This was accomplished by inserting the sweep voltage generator between the voltage supply controlling the primary energy (E_0 in Fig. 2) and the scattering chamber. The energy loss to be observed was set by means of the voltage supply E_L, which also determined the mean energy of the analyzer when the main (zero energy loss) beam was aligned. Energy-loss sweeps were made with the sweep generator in series with E_L.

[6] In particular, because of the constancy of the optics the effective output slit of the analyzer remains fixed and the area of an energy-loss peak will be proportional to the total current entering the analyzer for that peak; C. E. Kuyatt and M. E. Rudd, Bull. Am. Phys. Soc. 8, 336 (1963). Over a limited range of energy losses, then, the area of loss peaks, or their heights if the widths remain constant, will be proportional to the inelastic cross sections since the gas pressure, incident beam current, and effective collision volume remain constant. By scaling peak heights, relative cross sections have been measured for some of the principal energy losses in helium and argon for primary energies from 20 to 80 eV; G. E. Chamberlain *et al.*, *Abstracts of Papers Presented at the Fourth International Conference on the Physics of Electronic and Atomic Collisions* (Science Bookcrafters, Inc., Hastings-on-Hudson, New York, 1965), p. 378.

C. Threshold Operation

A second and major consequence of the revised spectrometer operation is that, to within the resolution of the apparatus, energy-loss peaks could be observed for incident energies ranging down to threshold. At threshold the low-energy electrons leaving the gas cell were accelerated to the analyzer and accelerated again to the collector, where they then had enough energy to be collected efficiently. The effective solid angle and collection efficiency as a function of energy near threshold were not known precisely since the three-element lens following the gas cell was not designed for threshold operation. However, this lens system, which is similar to the Soa type immersion lens,[7] has proved adequate for focusing onto the analyzer entrance plane the low-energy electrons leaving the scattering chamber.

In operating the apparatus near threshold, the lens between the gas cell and analyzer had two focusing modes. In the $+E0$ mode the potential of the electrode $E0$ (Fig. 1) was not changed significantly in readjusting from the main beam to an inelastic peak, so that for the $n=2$ helium loss peaks there was an approximately 20 V increase in potential for electrons leaving the gas cell. In the $-E0$ mode, electrode $E0$ was operated at a potential more negative than the mean analyzer potential. In the $+E0$ mode the adjustment of $E0$ for maximum signal was noncritical within a few volts. In the $-E0$ mode this adjustment was more critical, but there was no difference in the setting over the range of primary energies that was used. Essentially the same

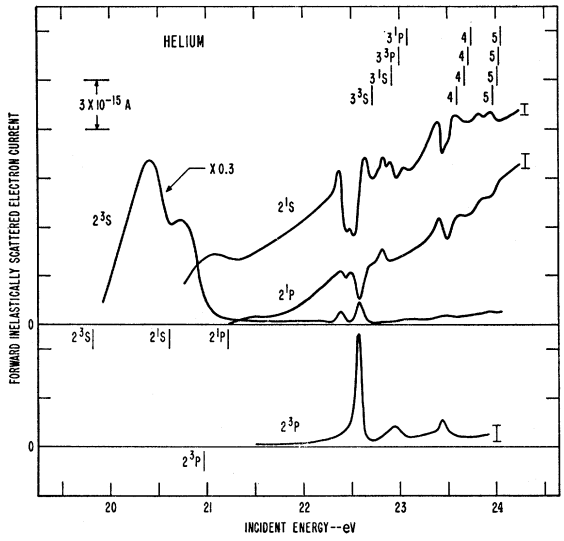

FIG. 3. Energy dependence of the forward inelastically scattered electron current in helium. Each curve is labeled according to the level excited and is a smoothed tracing from the original data. Noise width of the recorder traces is indicated by error bars. Details of the threshold portion of the $2^{3,1}S$ curves are shown in Fig. 5.

[7] J. A. Simpson, Rev. Sci. Instr. 32, 1283 (1961).

results were obtained in both modes, except for the region within 0.1 eV of threshold.

D. Resolution

It is interesting to note that for primary-energy sweeps the resolution will in principle be better than that of either the monochromator or analyzer, since the energy selectors are equivalent to two pass bands in series. For a Gaussian distribution and a resolution ΔE in each selector, the combined resolution is $\Delta E/\sqrt{2}$. When the analyzer is used to scan the output of the monochromator in the energy-loss mode the width at half-maximum will be $\Delta E\sqrt{2}$. That is, the over-all resolution in the primary-energy mode should be one-half of the resolution in the energy-loss mode.

The discrete-energy-loss peaks reflect the primary beam shifted in energy and, therefore, one might expect them to have the same width as the main beam. However, it was found that the energy-loss peaks are broader than the main beam by nearly a factor of two, probably because of small-angle scattering in the gas cell. This broadening resulted in the resolution of the primary-energy mode being comparable to the width of the observed main beam.

Small-angle scattering would allow electrons leaving the gas cell to have been scattered through an angle greater than that defined by the entrance and exit apertures. Since the resolution of the energy selector depends in part on the square of the incident-beam angle, it is estimated from the increased width of the loss peaks that the maximum observed scattering angle was less than 0.1 rad.

E. Operating Pressure

The operating pressure within the gas cell was adjusted to maximize the energy-loss peaks for $E_0=22$ eV. The strength of the energy-loss signal will go through a maximum since the gas density increases linearly with pressure while the loss of electrons, both primary and energy-loss, from the beam increases exponentially with pressure. Lassettre[8] has made a detailed analysis for an inelastic collision path length short compared to the attenuation path length.

For zero-angle scattering in a static gas we make the simplifying approximations that the collision volume is a right circular cylinder (length l) defined by the entrance-exit apertures and that the solid angle of collection is a constant ($\langle d\Omega\rangle_{\rm av}$) which is an unspecified average over the scattering path length. Denoting the differential cross section for inelastic scattering as σ_i, the total scattering cross section for primary electrons as $\sigma_1=\sigma_t(E_0)$ and for energy-loss electrons as $\sigma_2=\sigma_t(E_0-E_L)$, and the primary current as I_0, then the fraction of scattered electrons leaving the gas-cell is

$$I_i/I_0=\rho\sigma_i l\exp(-\rho\bar{\sigma}l)F(y)\langle d\Omega\rangle_{\rm av}, \qquad (1)$$

where ρ is the number density of the gas, $\bar{\sigma}=\frac{1}{2}(\sigma_1+\sigma_2)$, $F(y)=y^{-1}\sinh(y)$, and $y=\frac{1}{2}\rho(\sigma_1-\sigma_2)l$.

In the limit of $y\to 0$, $F(0)=1$ and I_i/I_0 has a maximum for $\rho\bar{\sigma}l=1$. The electron mean-free-path, then, is equal to the length of the scattering chamber and the main beam is reduced by $1/e$ from the zero-pressure value. This is consistent with the present experiments in which the main beam was found to be attenuated by approximately a factor of three at the operating pressure used.

In fact, the cross sections σ_1 and σ_2 are not equal under the conditions of the present experiment. Recently, Golden and Bandel[9] measured the absolute total cross section for e-He scattering from 0.3 to 28 eV. The cross section decreases monotonically (except for the 19.3-eV resonance) from a maximum of 5.6 Å^2 at 1.2 eV to 2.6 Å^2 at 20 eV. This 50% change in cross section has little effect on the criterion that $\rho\bar{\sigma}l=1$ for maximum signal since there is only a 2% increase in F from its limit value of 1.0, when $\rho\bar{\sigma}l=1$. From the modified effective-range formulation of O'Malley,[10] Golden and Bandel extrapolated their data and estimated the cross section at zero energy to be 4.68 Å^2. The effect of this 16% decrease from the maximum value on the currents observed is of little consequence here in view of the other uncertainties in the collection efficiency. Of more importance is the fact that the total cross section appears to be smoothly varying for both the primary and energy-loss electrons and therefore will not contribute to the structure seen in the cross-section curves.

III. DISCUSSION OF RESULTS

A study of the energy dependence for the excitation of the $n=2$ states of helium was made for incident energies between 19 and 24 eV. The X-Y recorder traces were made of the detected electron current as a function of incident energy for fixed energy losses of 19.82 (2^3S), 20.61 (2^1S), 20.96 (2^3P), and 21.22 (2^1P)eV.

The data shown in Figs. 3 and 4 were taken in the $+E0$ mode over a period of three days in which the apparatus operated very stably and reproducibly. The main beam current at a given energy did not vary more than 10% over this period. As a function of primary energy, the detected current had a broad maximum between 20 and 24 eV and it did not vary more than 30% over the same energy range. There was no provision to measure the total current entering the scattering chamber. Before and after each run the helium transmission peak near 19.3 eV was observed. The primary

[8] E. N. Lassettre and S. A. Francis, J. Chem. Phys. **40**, 1208 (1964).

[9] D. E. Golden and H. Bandel, Phys. Rev. **138**, A14 (1965).

[10] T. F. O'Malley, Phys. Rev. **130**, 1020 (1963).

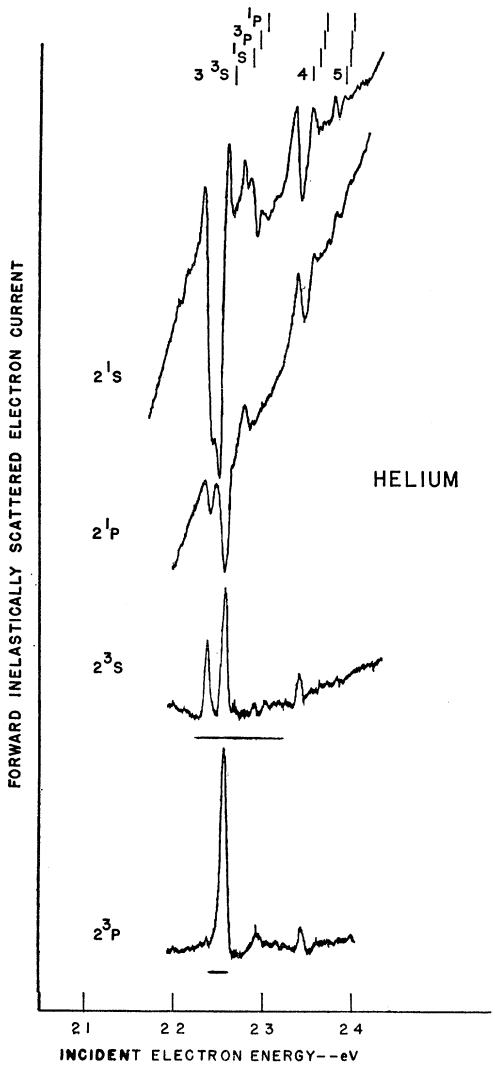

FIG. 4. Detail of resonance structure in helium from 22–24 eV. The curves are carefully traced from the original data. All but the smallest structure is reproducible. For example, the slight structure in the 2^1S curve at 22.1 eV is a noise pulse. The zero of cross section is arbitrarily displaced; for the 2^3S and 2^3P losses its position is indicated by the line under the corresponding curves.

energy scale was established by assigning a value of 19.31 eV to the transmission peak.[11]

A. 22–25 eV

Figures 3 and 4 show that there is considerable resonance structure present in the helium $n=2$ inelastic cross sections between 20 and 25 eV. The role of short-lived, intermediate, negative-ion states in causing interference with the direct excitation of the final state is now well established.[12] In Figure 3 the grouping of resonance structures above 22 eV is clearly associated with He^- states formed from the $n=3$, 4, and 5 levels of helium. It is interesting to observe that there are two series of He^- states which produce the stronger resonances. No doubt these involve one or more of the $(1s,ns^2)$, $(1s,ns,np)$, or $(1s,np^2)$ configurations. This double series of resonances had previously appeared as a small variation in the total cross section[2] and illustrates the amplification that in certain cases can be obtained by looking for resonance structure in the inelastic channels.

In Fig. 3 the peaks at 22.42 and 22.60 eV in the 2^3S curve and 22.60 eV in the 2^3P curve should be near the resonance energy of two of the negative ion states since the potential scattering is small. The observed linewidths appear to be limited by an effective instrumental resolution of <0.06 eV. Within the noise limitations of the apparatus, no peak could be seen in the 2^3P loss curve at 22.42 eV, indicating very little coupling of that particular He^- state to the 2^3P level.

The 22.4 and 22.6 eV resonances show up primarily as dips in the singlet cross sections, and the nearly 50% decrease in intensity in both the 2^1P and 2^1S curves are resolution limited. The small peak at the bottom of the 2^1S dip is considered not to be another resonance and is tentatively explained as follows. The lower energy resonance has a negative q line shape[13] (maximum followed by a minimum) and the higher has a positive q line shape (minimum followed by a maximum). It appears that the minima are sufficiently separated to leave a maximum between them. In Figs. 3 and 4 the pair of resonances move closer together for the $n=4$ and 5 states so that this intermediate maximum does not occur, or is not resolved.

B. 19.8–21.5 eV

The $^{3,1}S$ curves in Fig. 3 have a maximum several tenths of an eV above threshold. The large, broad peak with a maximum at 20.43 eV in the 2^2S curve is particularly outstanding; this curve is reduced by a factor of three relative to others. There is a shoulder on the side of the peak in the 20.6–20.8-eV range, and for the particular data shown, there appears to be a slight maximum at 20.7 eV. The 2^3S curve then drops precipitously to a small value above 21 eV. The peak height at 20.4 eV is in excess of 100 times the broad minimum in the cross section near 22.5 eV. The maximum in the 2^1S curve occurs at 21.1 eV. A measure of the uncertainty in the change in collection efficiency with primary energy is the fact that the 21.1 (2^1S) peak frequently appeared to be as large as the smooth part of the 2^1S curve near 22.5 eV.

In the data of Schulz and Philbrick for a scattering angle of 72°, the 2^3S curve rises to a peak near 20.4 eV that is about five times larger than the smooth part of the

[11] The value of 19.31 eV with an estimated limit of error of ±0.03 eV is given in Ref. 2. Additional published values include 19.30±0.05 eV (Ref. 1) and 19.285±0.025 eV (Ref. 9).

[12] P. G. Burke, Advan. Phys. **14**, 521 (1965).

[13] As defined by U. Fano, Phys. Rev. **124**, 1866 (1961).

curve at 22.5 eV, and there is a dip at 20.6 eV of about 50%. In the present experiment it is clear that at most there is a shallow minimum near 20.7 eV, although it is sometimes difficult to obtain the sharp features shown. The lack of a dip is understandable, because of the steep slope of the 2^3S curve for zero-angle scattering.

Recent calculations by Burke, Cooper, and Ormonde[14] confirm these observations and show that the various results for differential scattering at angles of 0° and 72° and for the measured total scattering cross sections[15,16] are consistent with one another. In the 2^3S curve the broad 20.4-eV peak is principally due to a ^2P resonance and partial waves with other angular momenta contribute little in this energy range. The inflection at 20.7 eV is caused by a ^2D resonance. Above 21 eV the S, P, and D waves in the 2^3S channel almost entirely cancel at zero angle, accounting for the observed decrease in the cross section.

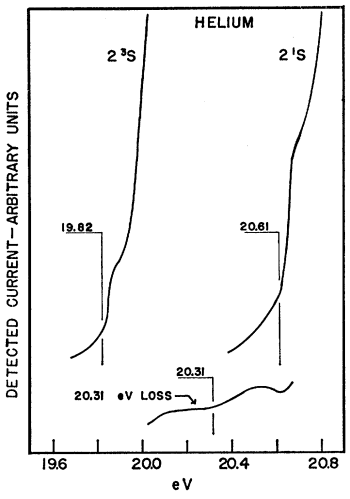

FIG. 5. Observed threshold energy dependence for excitation of the 2^3S and 2^1S helium levels by forward-scattered electrons. The zero of current is located arbitrarily in each curve. Behavior of the background current is shown by the middle curve for an energy-loss of 20.31 eV. The curves are smoothed tracings from the original data.

C. 2^3S, 2^1S Threshold Behavior

In a previous paper[4] it was mentioned that there appeared to be a sudden rise, or peak, in the 2^3S and 2^1S cross sections within 0.06 eV of threshold. Although it has been possible to reproduce the sharp rise in the cross sections, the design limitations and instability of the apparatus make it impossible to definitely exclude instrumental effects as a cause. In the earlier work there usually existed near threshold a small background of secondary electrons from the gas cell and a larger ~0.2-eV wide peak of electrons starting at threshold. The latter is attributed to direct scattering of the main beam from the exit aperture. Subtraction of this peak added to the difficulty of interpreting the earlier data. Since then it has been found that electrocleaning the molybdenum apertures briefly in KOH[17] helped eliminate the secondary-electron production.

Figure 5 shows data taken more recently than that in Figs. 3 and 4. The 2^3S and 2^1S loss curves exhibit a steep rise from threshold followed by an inflection before blending into the subsequent rise to a maximum several tenths of an eV above threshold. The magnitude of the initial rise in the 2^1S curve is about three times as large as that in the 2^3S curve, but relative to the following maximum in each curve the initial rise is ~3% for the 2^3S, and 20–30% for the 2^1S curve.

The 20.31-eV loss curve in Fig. 5 illustrates the technique for measuring the background electron current by adjusting the analyzer for an energy loss that does not occur in helium. The curve is essentially linear through threshold, and the fluctuations shown are caused by apparatus instability. Beneath the steep rise at threshold, the 2^3S and 2^1S curves are smeared out from ~0.2 eV below to ~0.1 eV above threshold. This is explained as being due to an observable amount of inelastic scattering occurring outside the exit aperture which was caused by the combination of the acceleration of the primary beam leaving the gas cell and the rapid increase of the cross sections above threshold.

There has been considerable concern as to whether the structure at threshold was instrumental in origin, but it is concluded that there is real structure in the cross sections within 0.08 eV of threshold. It has been impossible to construct a mechanism that would account for the observed shapes based on apparatus geometry, and in general, apparatus difficulties lead to a poorer resolution. Moreover, some form of this structure has been observed under a variety of experimental conditions. The empirical fact, alone, that the structure at threshold does not have the same magnitude in the 2^3S and 2^1S curves, whereas the slopes of both curves above threshold are nearly equal and the operating conditions of the apparatus are practically identical, indicates that the observed structure is not entirely instrumental. However, it should be noted that data taken in the energy-loss mode for a series of fixed primary energies ranging through threshold was not consistent with the structure at threshold in the primary-energy sweep mode, but apparatus instabilities and the small signals involved made this point inconclusive.

In the earlier runs there was a 1.5-mm diam angle-limiting aperture following the gas-cell which was replaced later by a 1.0-mm diam aperture. There was little difference in the character of the data in Figs. 3 and 4 for each case. The apertures are too large to intercept the primary beam and any interference with the collection of wide-angle and low-energy electrons should not result in the sharp features seen in Fig. 5. There remains the question of the unknown potential distribution at the exit aperture. Since the molybdenum oxide surface, and its adsorbed gas molecules, suffers a concentrated bombardment of 20-eV electrons and

[14] P. G. Burke, J. W. Cooper, and S. Ormonde, Phys. Rev. Letters **17**, 345 (1966).
[15] G. J. Schulz and R. E. Fox, Phys. Rev. **106**, 1179 (1957).
[16] H. K. Holt and R. Krotkov, Phys. Rev. **144**, 82 (1966).
[17] F. Rosebury, *Handbook of Electron Tube and Vacuum Techniques* (Addison-Wesley Publishing Company, Inc., Reading, Massachusetts, 1965).

metastable helium atoms, there may be a local change in potential that is not reflected as an energy spread in the 19.3-eV helium resonance. However, a compensating effect is the estimated on-axis increase in potential of 0.1–1.0 eV at the exit aperture due to the external accelerating field. Moreover, data have been taken in which an 0.1-eV wide peak of secondary electrons, believed to be generated at the exit aperture, occurred at an "apparent" 0.1 eV below threshold. In this case the onset in the 2^1S curve still appeared to be three times larger than in the 2^3S curve.

IV. CONCLUSION

A study of the energy dependence of the zero angle inelastic scattering of electrons by excitation of the $n=2$ levels in helium has shown clearly many narrow resonances (<0.03-eV wide) due to negative-ion states formed by attachment of an electron to the higher atomic levels ($n \geqq 3$). These resonances, and in particular a double rydberg series of levels, have appeared previously in total-cross-section measurements. Between the 2^3S and 2^1P thresholds there is broader resonance structure with the large peak in the 2^3S loss curve being about 0.5-eV wide. Extension of the $n=2$ loss curves to higher energy reveals resonance structure due to the He^- states at 57.1 eV $[(2s^22p)^2P^\circ]$ and 58.2 eV $[(2s2p^2)^2D]$.[18] Above this energy, decay to the doubly excited states of helium is dominant and no structure is seen. Both the 2^3S and 2^1S loss curves exhibit a sudden rise at threshold that is interpreted to mean that there is structure in the $2^{3,1}S$ excitation cross sections within 0.08 eV of threshold.

Application of the present technique to argon has not proved successful. Below the single ionization threshold the $4s\,^3P_1^\circ$(11.62 eV) and $4s\,^1P_1^\circ$(11.23 eV) losses were too small to be observed. In the 25–29-eV range, where the inner shell excited levels $3s \rightarrow ns$, np, and nd exist, no structure was seen.

ACKNOWLEDGMENTS

The author wishes to thank Dr. U. Fano, J. Cooper, and members of the Electron Physics Section for their suggestions and criticisms. He is also indebted to Dr. H. G. M. Heideman for his assistance in taking and interpreting experimental data.

[18] See Ref. 2. A study of the dependence on angle of these resonances has been made by J. A. Simpson, M. Menendez, and S. R. Mielczarek, Phys. Rev. **150**, 76 (1966).

PHYSICAL REVIEW VOLUME 155, NUMBER 1 5 MARCH 1967

Atomic Bethe-Goldstone Equations. I. The Be Atom

R. K. NESBET
IBM Research Laboratory, San Jose, California
(Received 27 October 1966)

The nonrelativistic electronic energy of Be(^1S) is computed by a generalization of the method of Brueckner, through the variational solution of generalized Bethe-Goldstone equations. These equations describe clusters of two, three, or four electrons interacting with the remainder of an N-electron system. The three- and four-particle terms are found to be very small, but the sum of three-particle terms is nearly 0.001 atomic units (a. u.). The computed correlation energy is −0.0921 a. u., or 98.1% of the difference between experimental total energy and computed Hartree-Fock and relativistic energies.

I. INTRODUCTION

IN recent years, it has become possible to carry out reasonably accurate electronic Hartree-Fock (HF) calculations on small molecules as well as atoms. This work has recently been reviewed.[1] As had been anticipated on theoretical grounds, the gross electronic density is quite well approximated by a HF wave function. However, electronic correlation, which is by definition neglected in the traditional HF approximation, contributes a large fraction of the energy difference between a molecule and its component atoms. Although evaluation of the correlation energy is the most obvious need, it is also desirable to be able to compute some one-electron properties of electronic systems with greater accuracy than is possible in the HF approximation. A striking example is the problem of the magnetic hyperfine coupling constant of the phosphorous atom in its ground state. Calculations based on the HF approximation get a result of opposite sign to that observed.[2]

The present paper will be concerned with a new method for computing correlation effects, based on successive variational solution of effective Schrödinger equations for clusters of one, two, three, etc., particles, embedded in the Fermi sea of the remaining particles of an N-fermion system. These equations, referred to as *n*th-*order* Bethe-Goldstone (BG) equations, are a gen-

[1] R. K. Nesbet, in *Advances in Quantum Chemistry*, edited by P.-O. Löwdin (Academic Press Inc., New York, 1966), Vol. III, pp. 1–24.

[2] N. Bessis, H. Lefebvre-Brion, C. M. Moser, A. J. Freeman, R. K. Nesbet, and R. E. Watson, Phys. Rev. **135**, A588 (1964).